JOURNAL OF GEOPHYSICAL RESEARCH, VOL. 106, NO. A6, PAGES 10,537–10,551, JUNE 1, 2001

Vertical wind observations with two Fabry-Perot interferometers at Poker Flat, Alaska

M. Ishii

Communications Research Laboratory, Ministry of Posts and Telecommunications, Koganei, Japan
Geophysical Institute, University of Alaska Fairbanks, Fairbanks, Alaska

M. Conde, R. W. Smith, and M. Krynicki

Geophysical Institute, University of Alaska Fairbanks, Fairbanks, Alaska

E. Sagawa and S. Watari

Communications Research Laboratory, Ministry of Posts and Telecommunications, Koganei, Japan

Abstract. Characteristics of vertical winds in the polar thermospheric region were examined using data sets generated with two types of Fabry-Perot interferometers at Poker Flat, Alaska (65.11°N, 147.42°W). The Communications Research Laboratory Fabry-Perot Interferometer (CRLFPI) simultaneously observed the O I 557.7 nm and O I 630.0 nm emissions, whereas the Geophysical Institute Scanning Doppler-Imaging Interferometer (GI-SDI) observed the O I 630.0 nm emission. The height of the O I 557.7 nm and O I 630.0 nm emissions were 100–140 and 200–240 km, respectively. The data were obtained from October 1998 to February 1999, and our findings were as follows: (1) Observations of the O I 630.0 nm emission showed that upward (downward) vertical winds were often present when bright aurora existed equatorward (poleward) of the observatory. This is consistent with previous studies [*Crickmore et al.*, 1991; *Innis et al.*, 1996, 1997]. (2) Comparison of vertical winds estimated from two different wavelengths (557.7 and 630.0 nm) showed that vertical winds were often observed simultaneously at both wavelengths, as reported by *Price et al.* [1995]. However, the vertical winds observed at different heights sometimes had different features when thin but bright aurora passed over the observatory. A similar observation was reported by *Ishii et al.* [1999]. (3) Vertical winds were often observed along with divergence and rotation of the horizontal wind field. Some vertical winds not associated with active aurora may be driven by the divergence in the horizontal wind.

1. Introduction

Since the unexpected observation near the auroral zone of strong vertical winds with velocities greater than 100 m s^{-1} [*Rees et al.*, 1984a], many studies have examined this phenomenon [*Peteherych et al.*, 1985; *Crickmore et al.*, 1991; *Price and Jacka*, 1991; *Conde and Dyson*, 1995; *Aruliah and Rees*, 1995; *Smith and Hernandez*, 1995; *Price et al.*, 1995; *Innis et al.*, 1996, 1997; *Ishii et al.*, 1999]. Vertical winds in the thermosphere can play a significant role in determining the thermospheric composition, large-scale circulation, and energy balance. For example, *Conde and Smith* [1998] suggest that horizontal winds in the *F* region may be deflected by upwelling vertical winds driven by *E* region heating in the auroral region.

Sources of thermospheric vertical winds have been studied by numerical techniques. *Walterscheid et al.* [1985] showed the effect of Joule and particle heating on wind systems near a single arc. *Rishbeth et al.* [1987] suggested two possible sources of vertical winds: a "barometric" component that includes the effects of heating and cooling of the thermosphere and a "divergence" component necessitated by the requirement of mass continuity. For downward winds, a lower altitude sink or cooling region and downwelling as part of a large-scale circulation system [*Rees et al.*, 1984b] are convincing possibilities.

Some studies have found possible relationships between vertical winds and the location of the auroral oval. *Crickmore et al.* [1991] estimated the upper thermospheric wind from the O I 630.0 nm emission measured with a Fabry-Perot interferometer (FPI) at Halley Bay, Antarctica. Their results indicated strong vertical winds of up to 50 m s^{-1} when the station was under the equatorward edge of the auroral oval. On the other hand, *Innis et al.* [1996, 1997] observed the O I 630.0 nm emission with a FPI at Mawson, Antarctica, and found many cases of upward vertical winds poleward of the poleward boundary of the visible auroral oval.

The wind velocities and temperature of the upper thermosphere are estimated from the Doppler shift and broadening of the O I 630.0 nm emission, respectively. Studies have also attempted to estimate the wind velocities and temperature of the lower thermosphere from the O I 557.7 nm emission despite the difficulties associated with an uncertain emission height and the large wind shears which can exist in the vicinity of the emission layer. *Price and Jacka* [1991] observed this emission from Mawson, Antarctica, and compared their results to spaced-antenna partial-reflection radar data. They concluded that strong upward winds (~30 m s^{-1}) at altitudes of less than 110 km appear to be a direct response of the neutral

Paper number 2000JA900148.
0148-0227/01/2000JA900148$09.00

atmosphere to an intense auroral event. The higher-altitude vertical winds were also measured but were not associated with particular events. *Price et al.* [1995] measured the O I 557.7 nm and O I 630.0 nm emissions from Poker Flat, Alaska. They found significant upwelling events in both the upper and lower thermosphere, and they developed a simple model, based on results from one case, to describe vertical wind systems near auroral arcs. *Ishii et al.* [1999] measured the O I 557.7 nm and O I 630.0 nm emissions from Ramfjordmoen, Norway, and observed clear phase differences in the vertical wind between the upper and lower thermosphere.

The theoretical relationship between horizontal and vertical winds based on the continuity equations was described by *Burnside et al.* [1981]. *Smith and Hernandez* [1995] calculated the correlation between vertical winds and the horizontal winds divergence by using observational data. Their results showed a relationship opposite to that of *Burnside et al.* [1981], which they attributed to different sources of divergent flow. While *Burnside et al.* [1981] considered the divergence of horizontal winds to be the origin of vertical winds, *Smith and Hernandez* [1995] postulated that it is the vertical winds and their vertical structure which cause the horizontal winds to diverge. *Ishii et al.* [1999] also considered these two relationships, with an emphasis on their time lag. Their findings were consistent with those of *Smith and Hernandez* [1995], with a time lag of ~10 min between the vertical wind and the divergence of the horizontal winds. A detailed review of other vertical wind studies was provided by *Innis et al.* [1996].

Our present study concerns vertical wind events observed through two independent FPIs from Poker Flat, Alaska (65.11°N, 147.42°W, in geographic coordinates; 65.4°N, 100.7°W, in geomagnetic coordinates), from November 1998 to February 1999. The local time in Alaska is 10 hours behind the universal time. One FPI (Communications Research Laboratory Fabry-Perot Interferometer (CRLFPI) [*Ishii et al.*, 1997]) had a narrow field of view (1.4° full angle) and observed emissions in only the zenith direction during the period. The other FPI was a Doppler-imaging etalon-scanning FPI (Geophysical Institute Scanning Doppler-Imaging Interferometer (GI-SDI) [*Conde and Smith*, 1995, 1997, 1998]), which could be used to estimate the horizontal vector wind field and temperature distribution in the field of view, as well as the vertical wind. The vertical wind is often weak and comparable in magnitude with errors from instrument instabilities and photon statistics. This makes the vertical wind difficult to estimate and may be a reason why previous studies only took extraordinarily strong vertical winds into account. We could defect weak vertical winds by comparing the results from the two independent FPIs, and we could deduce the relation between vertical winds and the divergence and rotation of the horizontal wind field. Furthermore, the CRLFPI measured the O I 557.7 nm and O I 630.0 nm emissions simultaneously so the vertical wind properties could be estimated at two different heights. From the O I 630.0 nm emission, temperatures were also estimated.

Simultaneous observations were made during new moon periods of the 1998–1999 winter, and we obtained measurements from 83 nights for the CRLFPI and 110 nights for the GI-SDI. The high temporal resolution (~2 min) of the CRLFPI was also an advantage, since vertical wind behavior is still not well understood and the circumstances surrounding each measurement may vary greatly. We also did a statistical analysis outlining the relation between vertical winds and auroral location. The auroral distributions were measured with a meridian-scanning photometer (MSP).

2. Instrumentation and Observations

The CRLFPI program consists of two types of FPIs, one having a narrow field of view and the other having a wide one [*Ishii et al.*, 1997]. The narrow field-of-view FPI (the scanning FPI) was installed at Poker Flat, Alaska, in September 1998. A single 116-mm aperture etalon with servo-control of the etalon spacing is operated at a 20.49-mm gap. The field of view is 1.4° full angle and is fixed to the zenith direction. Each fringe pattern image of the λ 630.0 nm and λ 557.7 nm emissions of atomic oxygen is recorded simultaneously on each of two output channels every 2 min. Each image has three orders of interference for 630.0 nm and four orders for 557.7 nm at the etalon. We used two kinds of laser for calibration: a He-Ne green laser (543.5 nm) for the shorter wavelength and a frequency-stabilized He-Ne red laser for the longer wavelength. We obtained one laser image every 10 observations (every ~20 min), which allowed us to characterize and correct for the effect of etalon gap drift. The wind velocities estimated from the images of both channels were also calibrated with the same frequency-stabilized laser. Generally, during a typical observing night, the fringe peak moved 1–2 pixels for a typical etalon gap drift, which corresponds to 70–140 m s^{-1} of wind velocity.

The Doppler "zero" velocity is difficult to determine in FPI observations. In this study, a one-night average of all vertical wind measurements was used to determine the zero Doppler shift, keeping in mind the possibility of a constant offset in wind variation. The same determination was used by *Price and Jacka* [1991], where the uncertainty of the Doppler "zero" velocity was usually less than 10 m s^{-1}. Also, when the observed aurora was too bright, the observation fringes were saturated, which can lead to overestimates of temperature and large errors in velocity. The maximum number of counts in 2 min was 1.206×10^6, so we did not use fringe images whose peak exceeded 1.10×10^6 counts to estimate temperature or velocity. Fortunately, such high intensities were seen only in the O I 557.7 nm emission. There was no saturation problem for the O I 630.0 nm emission.

The GI-SDI is based on a 100-mm aperture, capacitance-stabilized, Fabry-Perot etalon, the plates of which are piezoelectrically scannable in spacing over ~1.5 orders of interference (at λ 630.0 nm) about a nominal 20-mm gap. An all-sky lens and optical relay system maps an ~130° full angle field of view onto 5 orders of interference at the etalon. The instrument is configured to simultaneously measure line-of-sight winds from 25 independent zones mapping onto the sky as sectors of four concentric, annular rings centered about the zenith. The ring edges are spaced uniformly in terms of the zenith angle, with the outermost being at 65°, and the rings contain 1, 4, 8, and 12 sectors, respectively. The typical uncertainty concerning wind velocity is ~10 m s^{-1} when using an exposure time of 7 min. *Conde and Smith* [1995, 1997, 1998] give a detailed description of the instrument.

We applied a subsequent analysis to infer the two-dimensional vector horizontal wind field most likely to have yielded the observed azimuthal variation of the Doppler shift. To obtain the vector field, we assumed that for sufficiently short time intervals the rotation of the Earth can be regarded as moving the station through a meridional wind field that is stationary in local time. In our analysis we calculated the di-

vergence and rotation of the vector wind field. In general, FPIs can measure the divergence of a wind field but not the rotation. However, the above assumption permits us to estimate the rotation of the wind.

The GI-SDI normally does not monitor drift of its wavelength calibration during observations. (Usually, this is done by interrupting the sky observations with periodic observations of a calibration lamp.) The SDI etalon is very stable, with wavelength drift typically less than 10–20 m s^{-1} equivalent velocity over a night. Nevertheless, some attempt is made to remove even this drift. This is done by high-pass filtering the vertical wind data, on the assumption that the spatial and temporal average of the vertical wind should be small, over sufficiently large intervals. Thus the GI-SDI vertical winds shown here are effectively high-pass-filtered, to yield an approximately zero mean. The width of the filter window is quite large, up to 1/3 of the total data set.

The GI-SDI is intended mainly for measuring horizontal winds, which have greater speeds than vertical winds, and in this application the relatively crude method for removing etalon drift is quite adequate. However, for vertical winds the technique does introduce uncertainties that cannot be ignored. In consequence, it is only truly meaningful to compare the general shapes of the vertical wind variation in the two (CRLFPI and GI-SDI) instruments; the reader should not place much emphasis on comparing the absolute velocities recorded by each instrument.

In this study, our criterion for identifying vertical wind events was that the CRLFPI and the GI-SDI show similar wind behavior in the O I 630.0 nm observations. Because of this criterion, some events only detected through the O I 557.7 nm observations were not used.

For the given observation periods, auroral conditions were monitored using a meridian-scanning photometer (MSP), which recorded emission line intensities over 1° intervals along the magnetic meridian. In this study we used the two channels recording the intensities of the λ 630.0 nm and λ 557.7 nm atomic oxygen lines.

The principal emission height of each wavelength peak is dependent on the energy spectrum of the precipitating particles. The height of the O I 630.0 nm emission is ~200–240 km at the solar minimum, which is a nearly isothermal region [*Rees and Roble*, 1986]. However, under auroral conditions the O I 557.7 nm emission is mainly from the height range 100–140 km.

It is impossible to discuss Joule and particle heating as a source of vertical winds without having temperature measurements [*Rees et al.*, 1983]. However, the temperatures estimated from the FPI data in this study are difficult to use for this purpose, because energetic particle precipitation changes the auroral emission height [*Sica et al.*, 1996; *Price and Jacka*, 1991]. It is well known that when the auroral luminosity increases, the FPI-indicated temperature decreases in spite of the increased heating rate.

3. Results

In this section we describe 14 events of thermospheric vertical winds from four nights. The criteria for selecting events were (1) similar temporal wind variations indicated by GI-SDI and CRLFPI observations and (2) enough counts for precise fitting ($\geq 10^4$ counts) for CRLFPI. Since each event was identified from 630.0-nm measurements, the described features were not revealed by the 557.7-nm measurements. Errors shown for the CRLFPI and GI-SDI indicate uncertainty of one standard deviation in parameter estimates above and below the plotted point.

For each night the wind field divergence ($\partial u/\partial x + \partial v/\partial y$) and rotation ($\partial u/\partial y - \partial v/\partial x$) was calculated from the GI-SDI horizontal wind distribution results. Here we use positive divergence to imply a net outflow, corresponding to a source region, while negative divergence implies a net inflow or a sink region. Positive rotation means a counterclockwise flow when viewing the Earth from space.

The divergence showed very small value in our analysis. It comes from the assumption for obtaining a zero-velocity wavelength reference; in fact, the values shown here should be regarded as crude estimates only.

3.1. Case 1: November 25, 1998

The first case was observed on November 25, 1998. The *Ap* index for this day was 13. Two substorms were observed with onset times of 1215 and 1630 UT. The vertical wind events shown here were observed during the first substorm.

Plate 1 shows the results of the relevant quantities. Plate 1a shows auroral luminosities deduced from the CRLFPI observations at wavelengths of O I 630.0 nm (red) and O I 557.7 nm (green). Plate 1b shows the comparison of vertical winds estimated from the O I 630.0 nm observation with the CRLFPI (red) and with the GI-SDI (blue). Plate 1c shows the vertical wind measurements deduced from the two wavelength emissions, O I 630.0 nm (red) and O I 557.7 nm (green). Plate 1d shows the temperature variation of the O I 630.0 nm emitting layer. Plate 1e shows the divergence, $\partial u/\partial x + \partial v/\partial y$, in red and the rotation, $\partial u/\partial y - \partial v/\partial x$, in blue of the horizontal winds calculated from the vector wind estimation of the GI-SDI. The divergence estimate is relatively crude owing to the need to obtain a zero-velocity wavelength estimate from the data points themselves. Plate 1f shows the MSP observations of the 557.7 nm emission which identifies the relative location of bright aurorae.

We selected three periods from this date highlighted as "A," "B," and "C" in Plate 1c. Period A started at ~0840 UT. The magnitude of the wind deduced from the 630.0-nm emission was 20–30 m s^{-1} downward. Plate 1a shows that a small enhancement of the aurora corresponded with this period, and Plate 1d shows that the temperature estimated from the 630.0-nm emission decreased by ~100 K. This was an example of the height variation effect caused by energetic particle precipitation, as mentioned in section 2. A significant positive rotation was also observed just before this period, as shown in Plate 1e. When the wind rotation became almost zero, a bright aurora was seen north of the observatory. No significant features associated with the period were seen in the divergence.

Period B was from 1150 to 1215 UT. The GI-SDI data indicated a 50 m s^{-1} upward flow during this period, and the maximum velocity estimated from the CRLFPI data was 30 m s^{-1}. The winds calculated from the O I 557.7 nm emission showed similar features, but before and after the period a strong downward flow (40–50 m s^{-1}) was seen at the lower height. The 630.0-nm temperature (Plate 1d) did not vary significantly. The MSP data show the auroral arc moving equatorward of the observatory, at the end of period B, with the end of the upward flow corresponding to the poleward expansion. At this time both FPIs observed a steep downward shift in the

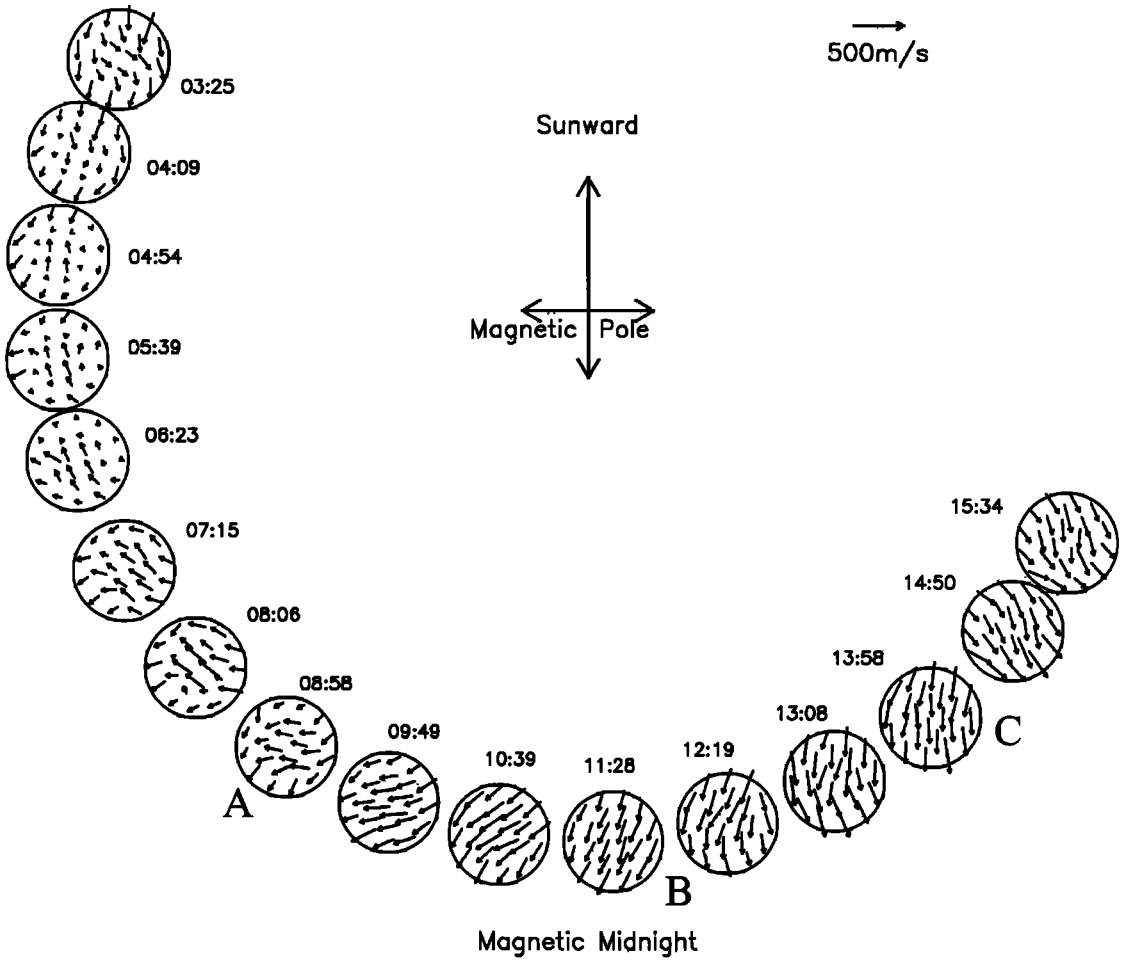

Figure 1. Evolution of the thermospheric horizontal vector wind field on the night of November 25, 1998. Times indicated are in UT.

vertical wind velocity: The rotation of the horizontal wind field also changed significantly at the end of this period.

Period C was from 1410 to 1435 UT. At this time the aurora moved poleward, and the intensity decreased. The wind velocity was 30 m s^{-1} downward. Significant variation was seen in the rotation of the horizontal winds.

Figure 1 shows a dial plot of the vector winds. This plot shows the time history of the vector wind field, in a geomagnetic coordinate frame, as seen by an observer looking down on the north geomagnetic pole of the Earth during the course of the night. The rotation of the Earth carries the observatory anticlockwise around the pole as seen by the observer. Although such plots can only show measurements every 40 min or so, the full time resolution of the original data was 8 min. Before period A, southward wind was observed equatorward of the observatory with southwestward flow seen in other regions of the field of view. After period A the wind vector magnitudes increased, and the wind vector directions became unified to the southwest. The directions gradually changed to the south, and after period B the southward wind was again observed south of the observatory but with the southwestward flow still seen in the other regions. This tendency continued to the end of the observation period.

3.2. Case 2: December 25, 1998

The second case was observed on December 25, 1998. The *Ap* index for the day was 12, but *ap* reached 27 between 0900 and 1200 UT. Magnetometer data from Poker Flat for this day was not available. Plate 2 shows the FPI results. The format is the same as that in Plate 1. Six periods were selected for this case.

In period D, upward flow was observed from 0925 to 0945 UT. The velocity estimated from the O I 630.0 nm measurement was 30 m s^{-1} (CRLFPI) and 60 m s^{-1} (GI-SDI). The absolute value of the O I 557.7 nm vertical wind estimation was small in this period but clearly accelerated in the upward direction from the downward flow observed before the period. The O I 630.0 nm temperature fluctuated but tended to rise. The rotation of the horizontal winds showed significant positive change with a time delay, but the divergence was stable. The MSP showed multiple auroral arcs moving equatorward before the period, with the brightness suddenly increasing during the period. When a thin arc passed over the observatory, the CRLFPI observed a sudden downward acceleration at both wavelengths. The upward velocities detected by the GI-SDI also decreased at this time.

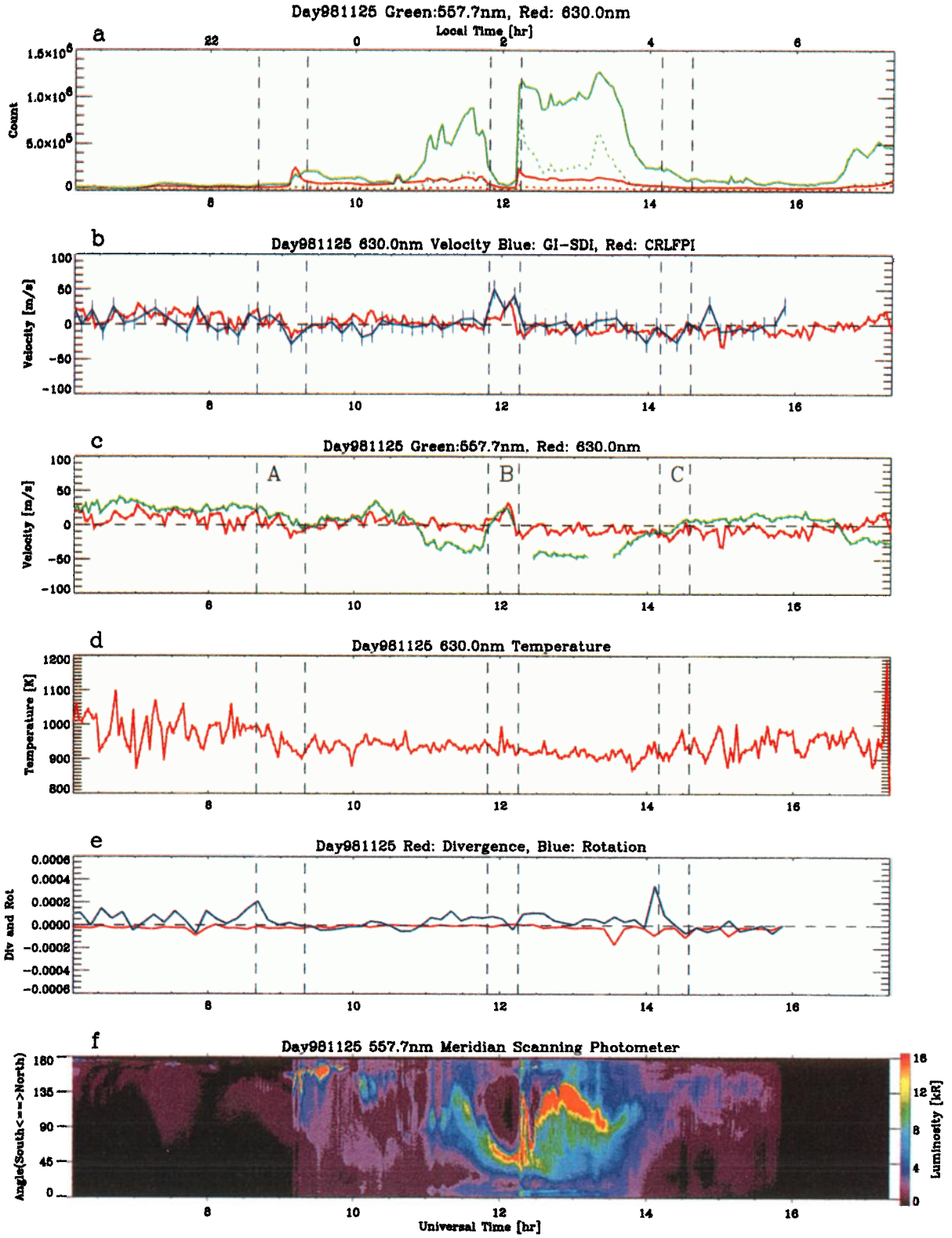

Plate 1. Wind and temperature variations estimated from Communications Research Laboratory Fabry-Perot Interferometer (CRLFPI) and Geophysical Institute Scanning Doppler-Imaging Interferometer (GI-SDI) data measured on November 25, 1998. (a) Peak (solid line) and background (dotted line) intensities of two emissions, O I 630.0 nm (red) and O I 557.7 nm (green) obtained by CRLFPI. (b) Comparison of vertical wind estimated from O I 630.0 nm measurements with two FPIs (blue, GI-SDI; red, CRLFPI). (c) Vertical wind velocity estimated from two emissions with CRLFPI (green, 557.7 nm; red, 630.0 nm). (d) Temperature estimated from 630.0-nm measurements with CRLFPI. (e) Divergence and rotation of horizontal wind calculated from GI-SDI measurements. (f) O I 557.7 nm auroral distribution obtained with a meridian-scanning photometer (MSP).

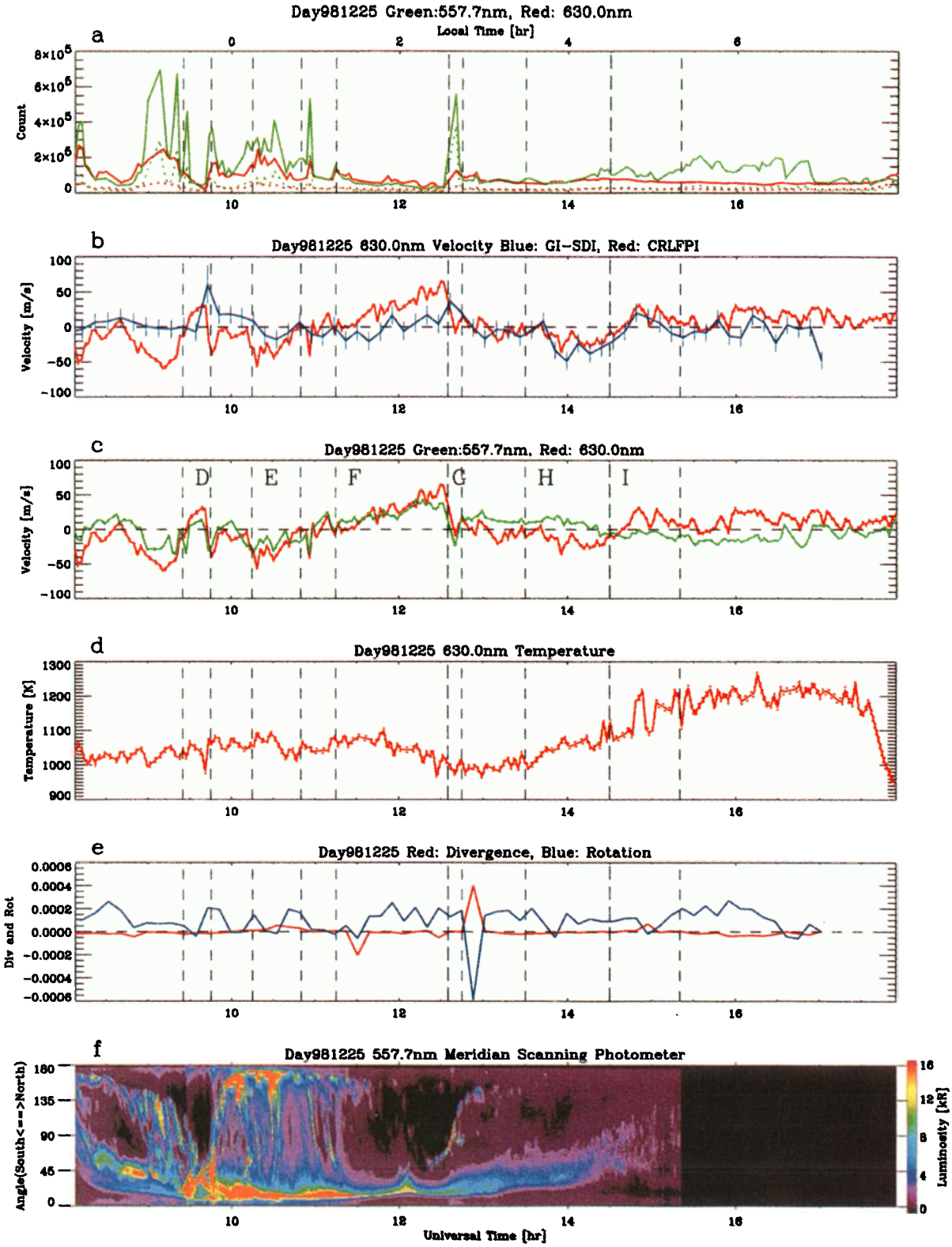

Plate 2. (a–f) Wind and temperature variations estimated from CRLFPI and GI-SDI data measured on December 25, 1998. The format is the same as that in Plate 1.

Period E was from 1015 to 1050 UT. Upon recovering from the sudden downward acceleration, downward winds were observed at both emission altitudes. For the O I 630.0 nm measurement the maximum wind magnitude was 60 m s^{-1} (CRLFPI) and 20 m s^{-1} (GI-SDI). For O I 557.7 nm the maximum velocity was 30 m s^{-1}. The O I 630.0 nm temperature decreased by ~100 K, and the divergence displayed temporal variation during this period. The MSP showed bright

aurora located both poleward and equatorward of the observatory. This auroral arc sometimes passed over the observatory. After the end of period E (just before 1100 UT), an arc passed over from poleward to equatorward. A fairly strong downward flow at both emission altitudes was indicated by the CRLFPI.

After period E, upward vertical winds gradually accelerated and reached 50 m s^{-1} (CRLFPI) and 30 m s^{-1} (GI-SDI) for O I 630.0 nm and 40 m s^{-1} for O I 557.7 nm by 1230 UT (at the end of period F). During period F, temperatures decreased gradually at the O I 630.0 nm emission height. After a large clockwise rotation during the recovery from period E, a very large anticlockwise rotation developed. At the beginning of the period a negative wind divergence was also seen.

Period G immediately followed period F. During this period, downward acceleration was observed in both CRL channels at 1240 UT. The velocity of the downward wind was 70 m s^{-1} at O I 630.0 nm and 50 m s^{-1} at O I 557.7 nm. The GI-SDI observation also showed a similar temporal variation. Auroral intensity was enhanced especially at O I 557.7 nm. The O I 630.0 nm temperature showed a local minimum just after the period. Both the divergence and the rotation changed significantly just after this period. During the period the MSP showed a relatively thin but bright auroral arc passing overhead.

There was a significant difference in the wind features indicated by the O I 557.7 nm and the O I 630.0 nm emission after period G. Prior to period G, both CRL wavelength channels showed similar vertical velocities. Following period G and until 1430 UT, the O I 557.7 nm channel showed a weak upward wind of 10–20 m s^{-1}, whereas the vertical velocity estimated from the O I 630.0 nm channel remained ~20 m s^{-1} less than this. At 1430 UT, the onset of period I, the relative difference between the O I 630.0 nm and O I 557.7 nm velocities reversed, so that the vertical wind velocity in the upper thermosphere continuously exceeded that in the lower thermosphere. This difference continued until the end of our observations, and during this time the sign of the wind velocities at both emitting heights changed.

Period H was from 1330 to 1430 UT. The GI-SDI and CRLFPI data showed very similar behavior, with a downward flow reaching a maximum velocity of 30–40 m s^{-1}. The O I 557.7 nm measurement showed a weak upward flow (20 m s^{-1}), and the wind changed to downward at the end of the period. The O I 630.0 nm temperature increased gradually during this period. The divergence showed no change, and the rotation of the horizontal wind remained positive except at one point, which was close to the time at which the maximum downward wind was observed. The MSP showed that a broad auroral arc approached the observatory but with a decreasing intensity.

Period I was from 1430 to 1520 UT. The O I 630.0 nm wind in this period became upward, with a velocity of 30 m s^{-1}. At O I 557.7 nm a weak downward wind was detected. The O I 630.0 nm temperature increased but with large fluctuations. A large positive rotation and a relatively small positive divergence were observed. One dip in rotation occurred, at the time of the maximum upward wind. No aurora was recorded by the MSP.

Figure 2 shows a vector plot of the horizontal winds estimated from the GI-SDI data for December 25, 1998. Just before period D, westward flows were detected poleward of the observatory, but equatorward of the observatory, the wind velocity was low. After period D the westward flow spread into the region where the wind velocity was low, and in period E the wind field changed to the southwestward direction east of the observatory. Near magnetic midnight, southward flow was dominant over the entire field of view, but after periods F and G a clear curvature was seen, with southwestward flow poleward of the observatory and southeastward flow equatorward. This structure persisted until the end of our observations, but with the wind velocity equatorward of the observatory becoming weaker after periods H and I.

3.3. Case 3: January 8, 1999

The third case was observed on January 8, 1999. The *Ap* index for this day (*Ap* = 17) indicated higher geomagnetic activity than for the previous cases, but *ap* was only 9 during the selected period. A medium-scale substorm onset occurred at ~0900 UT, and magnetic activity increased after 1200 UT. From this case we selected one period which is occurred before the substorm. Plate 3 shows the FPI results. Period J was characterized by an upward vertical wind from 0720 to 0810 UT. The maximum wind velocity from O I 630.0 nm data was 50 m s^{-1}. From O I 557.7 nm data the maximum was 20 m s^{-1}. The O I 630.0 nm temperature showed some fluctuation with an amplitude of ~100 K. The temporal variation in the divergence and the rotation was relatively uniform. The MSP showed a thin but bright auroral arc poleward of the observatory. Figure 3 shows a vector plot of the horizontal winds. The distribution at 0654 UT shows an eastward flow equatorward of the observatory and a weak northward flow poleward. This northward flow developed before period J, but the wind distribution was not uniform. This confusing condition continued until 0820 UT (after period J).

3.4. Case 4: February 11, 1999

The last case introduced here was observed on February 11, 1999. The *Ap* index for this day was 20. Local magnetometer data showed the onset of large-scale substorms at 1130 and 1500 UT. Four periods were selected from this case (Plate 4).

Period K was from 0840 to 0930 UT. The O I 630.0 nm data indicated upward vertical winds that lasted for 50 min with a maximum velocity of 40 m s^{-1} (CRLFPI). The O I 557.7 nm vertical winds were weak during this period. The O I 630.0 nm temperatures displayed no remarkable variations during this period. The horizontal wind rotation was generally positive with little variation. The divergence was almost zero. The MSP recorded a very weak auroral arc equatorward of the observatory.

Period L started at 1030 UT and ended at 1120 UT. An upward vertical wind occurred during this period, and the maximum velocity from O I 630.0 nm data was 30 m s^{-1}. Before period L, from ~0800 UT, the vertical winds estimated from O I 557.7 nm data and from O I 630.0 nm data clearly differed in behavior. However, their behavior became similar again during period L. The 630.0-nm temperature was stable. Before this upward wind period the rotation was positive. During the period the rotation became small, and after the period the rotation became weakly negative. The divergence was small throughout the period. The MSP showed that there was a bright aurora displaying fine structure above the observatory from 1000 to 1030 UT. The aurora moved equatorward during period L, and its intensity decreased.

Period M was characterized by a downward wind from 1200 to 1240 UT. The maximum velocity was at 30 m s^{-1}. The O I

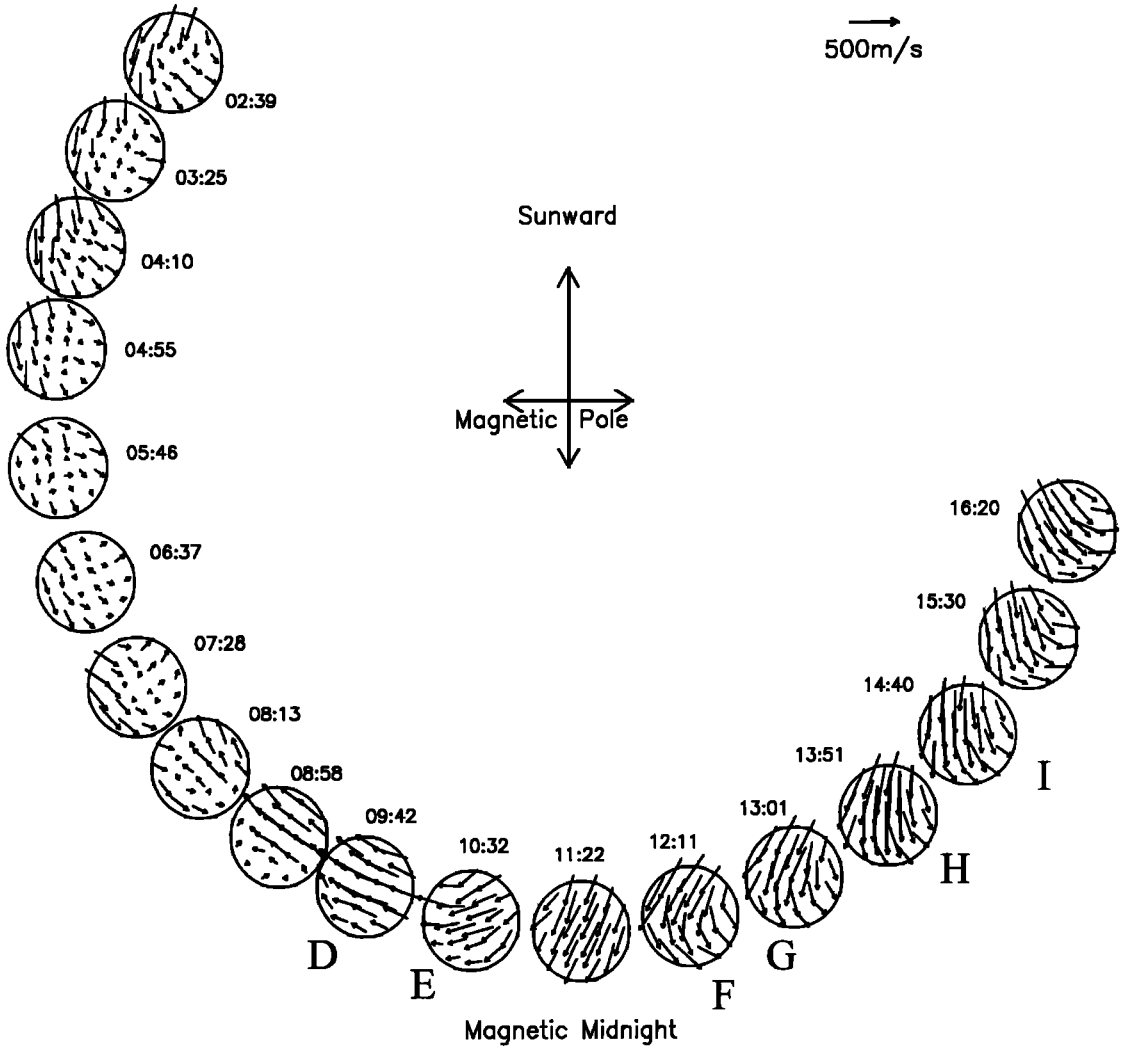

Figure 2. Evolution of the thermospheric horizontal vector wind field on the night of December 25, 1998. Times indicated are in UT.

557.7 nm data indicated a downward vertical wind before the period at ~1140 UT. The 557.7-nm luminosity sometimes rose above 1.1×10^6 counts per second (cps) during this period, and so we did not use the data for those times. The O I 630.0 nm temperature showed one peak during this period, and there was little variation in either the divergence or the rotation. After this period the rotation again increased. The MSP showed a broad auroral arc poleward of the observatory and that the auroral intensity above the observatory had increased.

During period N, from 1345 to 1500 UT, the CRLFPI data indicated fluctuating upward winds, with the maximum velocity reaching 50 m s^{-1} for O I 630.0 nm. The GI-SDI measurements indicated similar features (maximum of 30 m s^{-1}). The 557.7-nm measurements also showed similar features at the beginning of the period, but the velocity changed at ~1445 UT, turning negative and reaching 30 m s^{-1} downward at 1500 UT. The O I 630.0 nm temperature fluctuated slightly during the period, and the rotation was positive. There was an auroral arc equatorward, and it extended to the observatory after 1430 UT. At 1500 UT the arc broadened poleward.

Figure 4 shows a vector plot of the horizontal wind distribution for this case. At 0732 UT the wind direction was uniformly westward, but the velocities to the south were lower. By 0814 UT the velocities to the south had increased, and the vector map looked similar across the entire field of view. This tendency continued until after period K, and at 1100 UT (during period L) the wind field direction was southwest. The wind distribution remained uniform until 1143 UT, but the equatorward wind turned to the east after period M enhancing the curvature structure. This structure was seen until 1430 UT; then after period N the wind distribution became generally southward.

3.5. A Statistical Study of the Relation Between Vertical Winds and Auroral Location

Using the same criteria as that for the above cases, we selected 43 vertical wind periods obtained with the CRLFPI using the O I 630.0 nm emission from 16 nights between November 20, 1998, and February 15, 1999. There were 26 instances of upward vertical winds and 17 of downward winds. From these data we deduced a statistical relationship between vertical winds and the location of auroral arcs. The distributions of auroral luminosity along the magnetic meridian were averaged for two cases, upward and downward winds. The

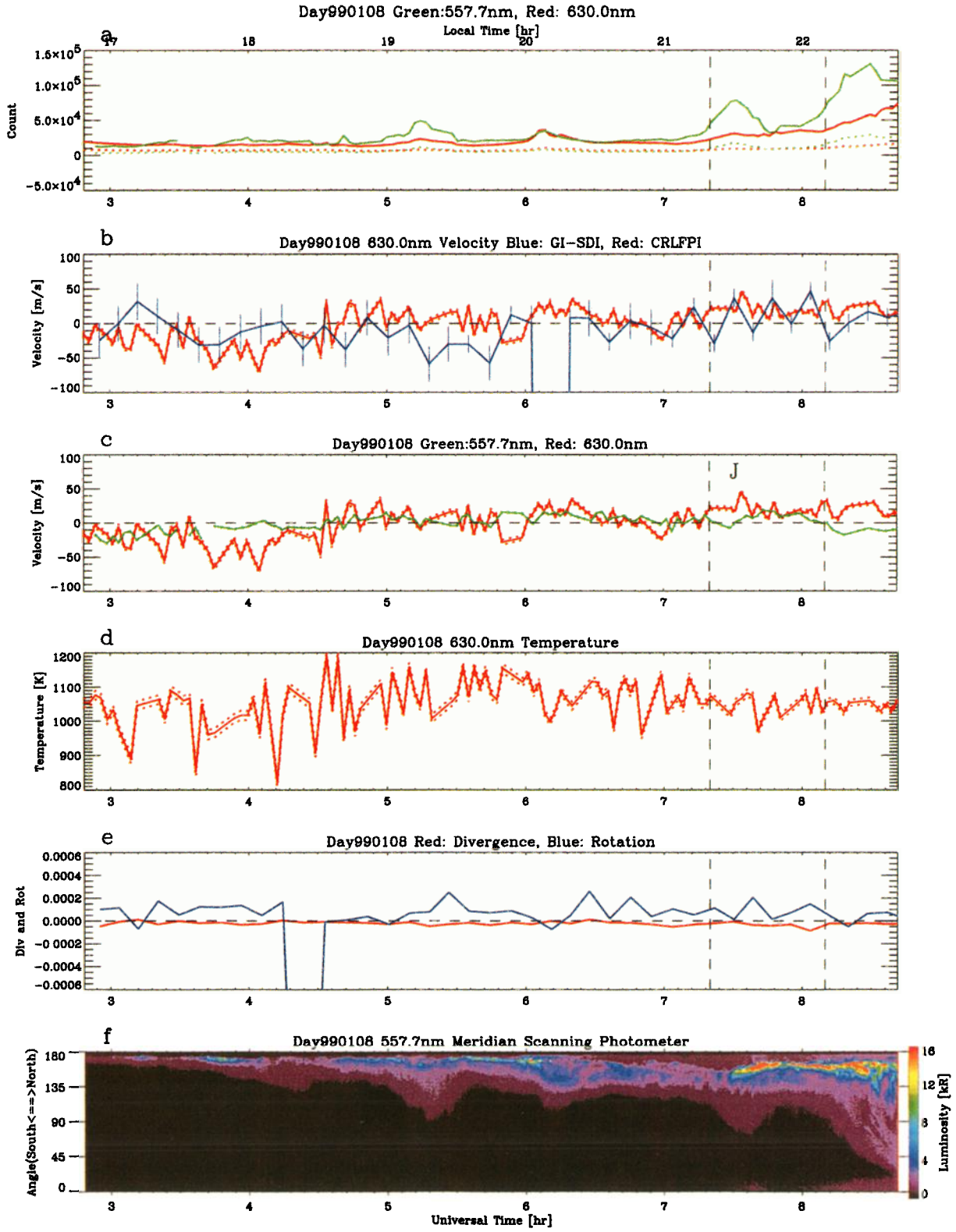

Plate 3. (a–f) Wind and temperature variations estimated from CRLFPI and GI-SDI data measured on January 8, 1999. The format is the same as that in Plate 1.

velocity of the vertical winds was not considered in this analysis. As a reference for this period, an averaged auroral distribution, regardless of the vertical wind, was calculated using MSP data from 19 clear nights. To derive this reference, the auroral luminosity versus the angle along the meridian was sampled at every hour from 0400 to 1500 UT and then was averaged. To estimate the variability of this profile, we repeated this procedure 19 more times. In these 19 other cases

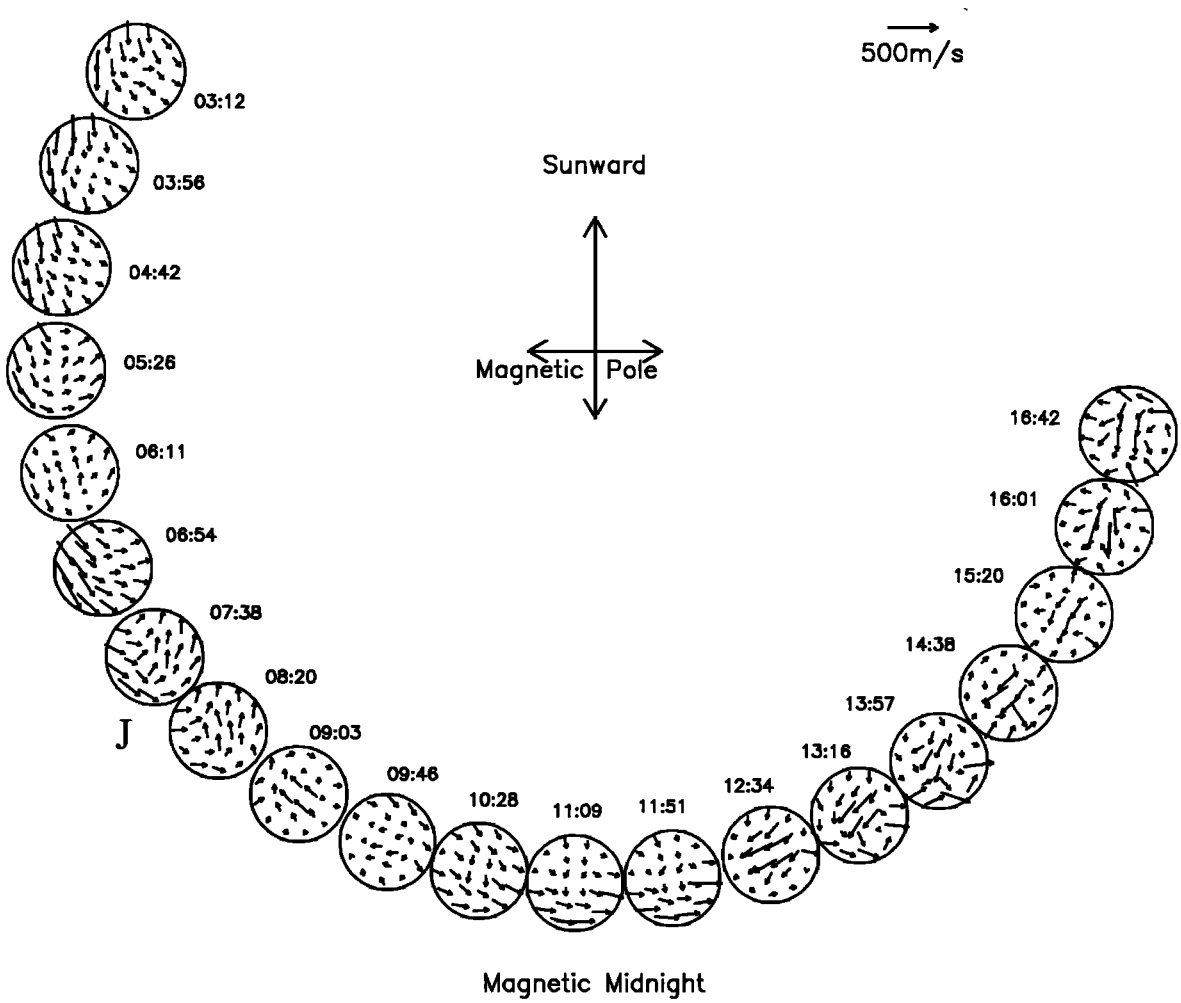

Figure 3. Evolution of the thermospheric horizontal vector wind field on the night of January 8, 1999. Times indicated are in UT.

the sample times were delayed by from 3 to 57 min (in 3-min steps) with respect to the hourly sampling in the first case. In total, this gave us 20 profiles of auroral luminosity versus angle along the meridian, which enabled us to calculate the standard deviation of luminosity at each scan angle. Figure 5 shows the results of this analysis. For Figures 5a and 5b, respectively, we used the O I 557.7 and O I 630.0 nm auroral luminosity measurements.

Figure 5a shows that the auroral distribution of both the downward wind and the averaged cases was quite different from the upward wind case. All three cases similarly showed two peaks, one poleward and the other equatorward of the observatory. However, when upward winds were observed, the poleward intensity peak was about half that of the other cases, while the equatorward intensity peak was slightly higher than the others. The poleward distributions for the downward wind and averaged cases were almost the same. The averaged value was higher than the downward value in equatorward, except at ~80° equatorward, where a peak in the downward wind exceeded the averaged value.

Figure 5b shows little difference among the three cases, in contrast to the 557.7-nm results. The poleward peak is dominant in each case. The upward winds produced the highest peak, but the difference was only 100–150 R. The averaged value was lowest for almost the entire meridional scan.

4. Discussion

4.1. Vertical Winds on a Large Spatial Scale

Our results show that the vertical wind features on a large spatial scale (approximately several hundred kilometers near auroras) differ from those on a small spatial scale (the same size as a single arc). Thus we will discuss these separately.

Previous studies have shown that downward winds in the upper thermosphere are often observed equatorward of auroral arcs and that upward winds are observed poleward of arcs [*Crickmore et al.*, 1991; *Innis et al.*, 1996, 1997]. Our results for 10 of the 14 periods are consistent with these studies; downward winds (periods A, C, and M) were observed equatorward of auroral arcs, and upward winds (periods B, D, F, I, K, L, and N) were measured poleward of the arcs. Our statistical study also showed this tendency. When upward vertical winds were observed, auroral luminosity on the poleward side of the observatory was weak, and luminosity on the equatorward side was stronger than the averaged auroral luminosity. Because the observatory was in a subauroral region (invariant latitude

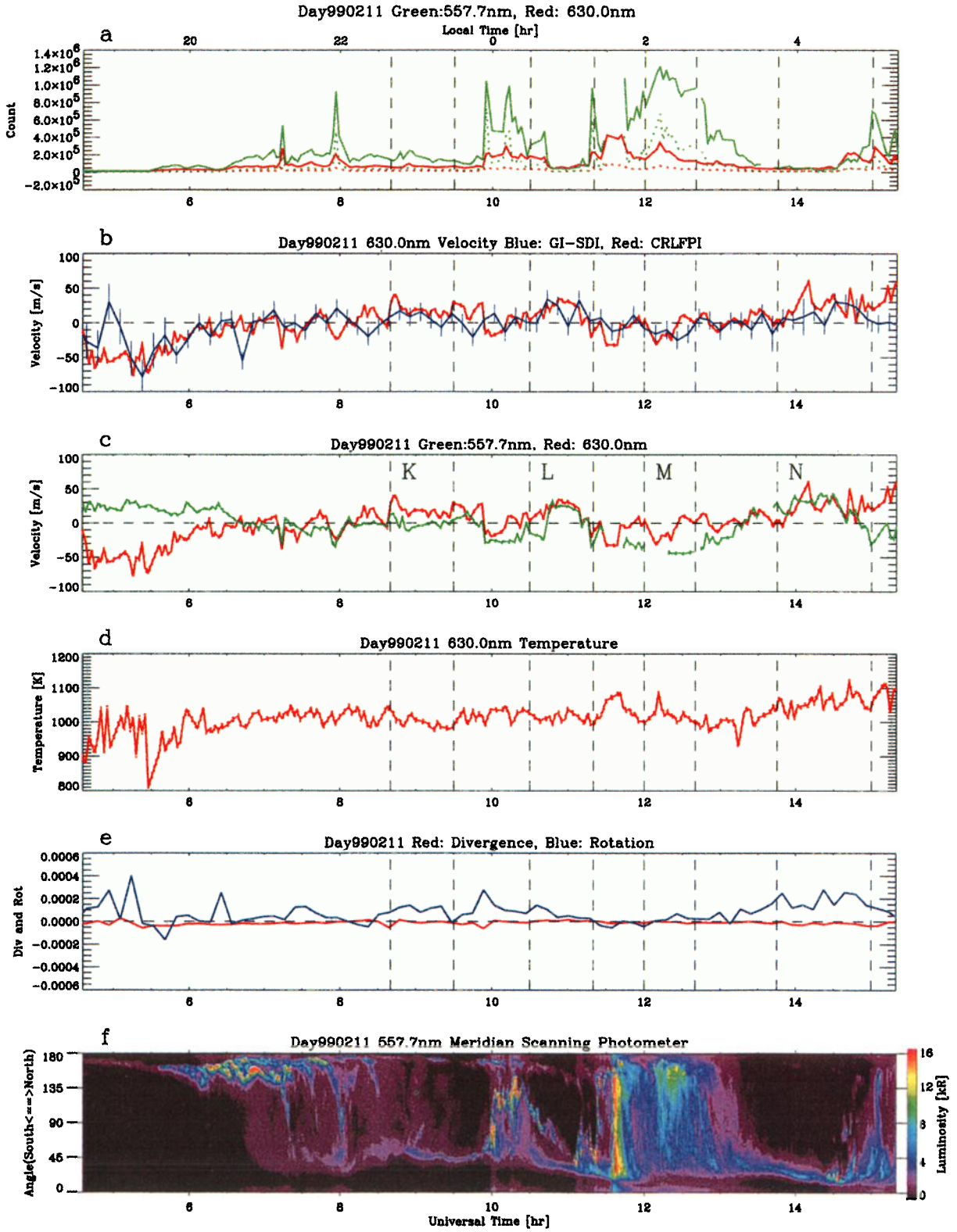

Plate 4. (a–f) Wind and temperature variations estimated from CRLFPI and GI-SDI data measured on February 11, 1999. The format is the same as that in Plate 1.

65°), the aurora was more often observed poleward of the observatory. Figure 5a shows no prominent differences in the auroral distribution between the downward wind case and the averaged case on the poleward side. However, decreased auroral luminosity to the equatorward side for the downward wind case agrees with the results of *Crickmore et al.* [1991], who showed downward winds equatorward of auroral arcs. The results shown in Figure 5 are consistent with the possibility that

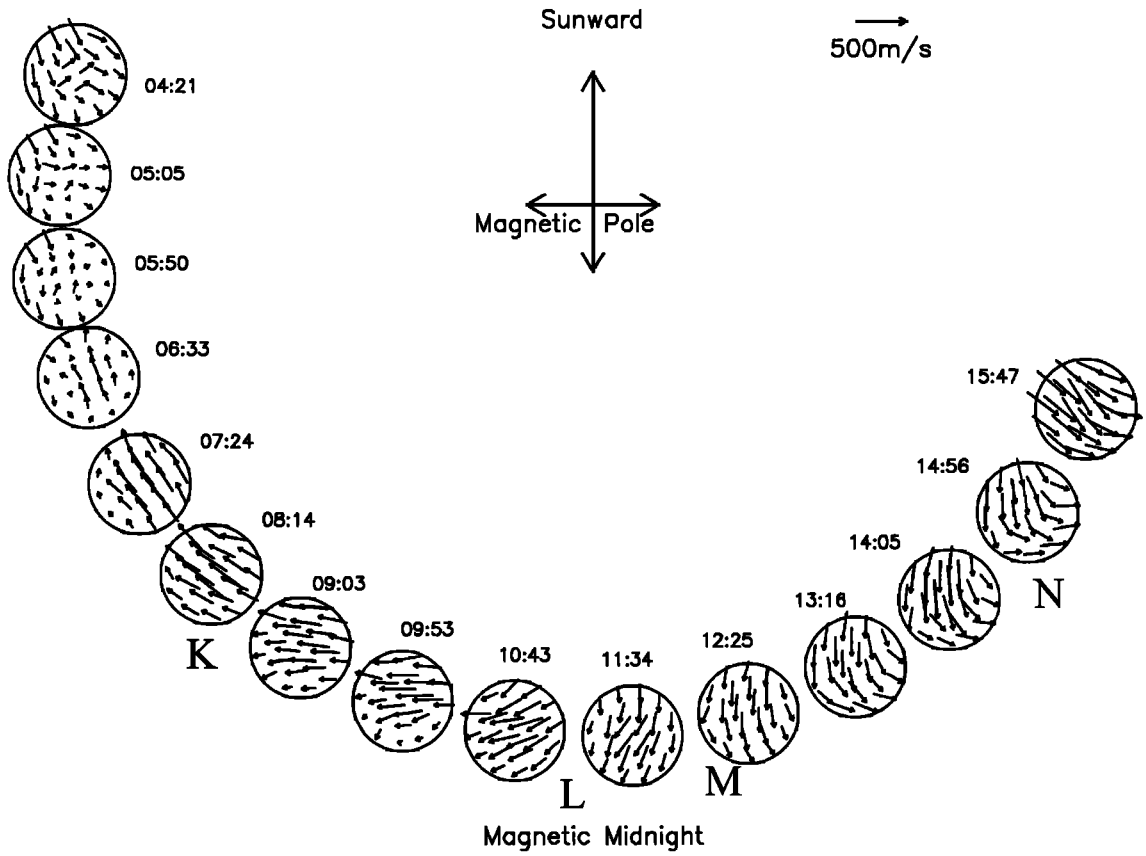

Figure 4. Evolution of the thermospheric horizontal vector wind field on the night of February 11, 1999. Times indicated are in UT.

Joule and frictional heating driven by auroral particles cause thermospheric vertical winds, but we have no direct evidence of this (e.g., a temperature increase), because of our lack of emission height information as explained earlier. Any Joule/frictional heating process near aurora would be complicated, and more detailed observations, theories, and computer simulations are needed to discuss such a process in detail. However, our results provide some meaningful preliminary information for such discussions.

Periods H and J clearly showed different features from the other periods. Downward flow was seen poleward of the auroral arc in period H, and upward flow was observed equatorward of the aurora in period J. As explained in section 2, the actual velocities and directions of the vertical winds were uncertain. However, the relative differences can be trusted, and these indicated that there must have been significant acceleration in both cases.

We consider the most reasonable vertical wind structures surrounding the auroral oval or large-scale auroral arcs to be as follows. Upward vertical winds are generated by Joule/particle heating in the auroral arcs, and downward flows occur on both sides of the arcs [*Rees et al.*, 1984b]. Recent studies have shown that Joule heating strongly affects the poleward edge of the auroral oval (R. Fujii, Nagoya University, private communication, 2000); then it is natural that upward flow also often occurs poleward of the oval [*Price et al.*, 1995]. Another recent study showed that the downward flow distribution is modulated by strong horizontal winds: Downward winds are enhanced on the downstream side (H. Shinagawa, Nagoya University, private communication, 2000). In many cases there are large equatorward winds, caused by solar UV heating, on the nightside of the region. This background horizontal wind may enhance downward flow equatorward of the auroral oval.

4.2. Vertical Winds on a Small Spatial Scale

During period G a thin but bright auroral arc passed over the observatory. This coincided with the observation of a large shift from upward to downward velocity, which was simultaneously seen in both the higher and the lower thermosphere. A similar case was seen at 0715 UT of February 11, 1999 (Plate 4c), although we did not mention it earlier because of its short duration. Significant differences in both wind magnitude and direction were indicated by both the O I 630.0 nm and the O I 557.7 nm measurements before and after these periods. Vertical wind measurements from both emission layers, obtained at Ramfjordmoen, Norway, revealed similar behavior [*Ishii et al.*, 1999]. In period G the auroral luminosities were slightly different before and after the auroral arc passed over the observatory (Plate 2).

These vertical winds on a small spatial scale seem to be driven by different physical processes from that on a large scale (described above), because the temporal/spatial variations in the small-scale wind velocity are very large compared with those of large spatial scale vertical winds. That the source of such vertical winds is Joule/particle heating sounds plausible, because these winds appear together with bright auroras. If the strong downward winds are generated by heating, the heat source would probably be above the emission layers and the

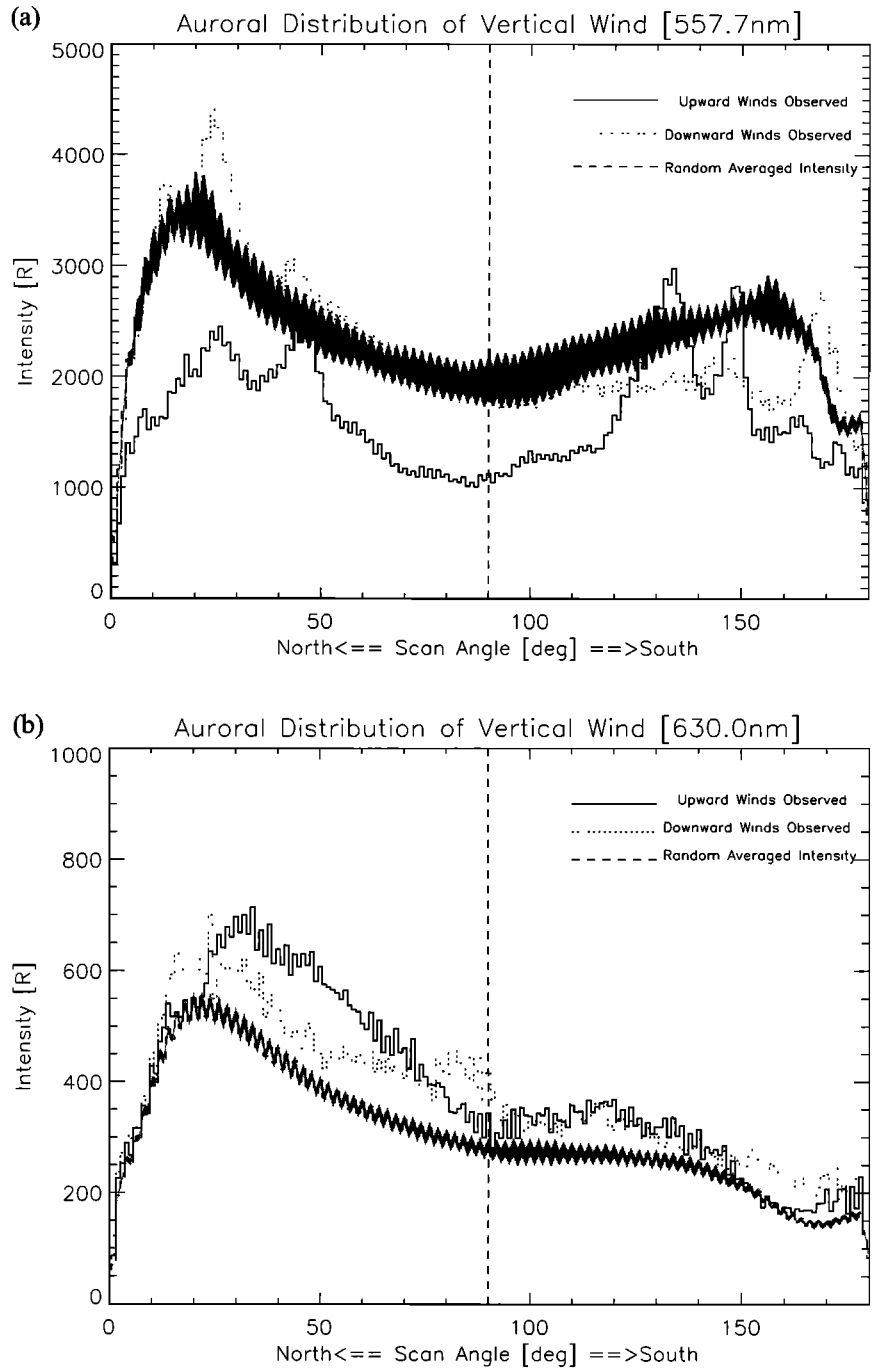

Figure 5. Statistical relationship between vertical winds and the location of auroras. (a) Averaged location of auroral O I 557.7 nm emission when upward (solid) and downward (dotted) winds were observed, and (b) the same format for O I 630.0 nm emission. Forty-three instances of vertical wind examples were observed from O I 630.0 nm measurements, obtained from November 20, 1998, to February 15, 1999.

neutral atmosphere would be accelerated downward by heat expansion. However, many theorists object to this idea: An extremely large energy input would be needed to generate downward winds in this way, because the thermospheric density exponentially increases with decreasing height. In addition, our results show that the vertical wind can occur simultaneously at two different heights. This means that a very tall pillar (>100 km) of air would have to be accelerated downward, and the heat source would have to be located in the upper thermosphere (≥240 km). This is difficult to believe, and we need other scenarios.

Another important feature of vertical wind behavior was observed in period G. Small-scale auroras near an observatory seemed to affect vertical wind behavior more strongly than did large-scale distant auroras, indicating that local sources are much more important to vertical wind phenomena. Of course, this is just one example, and other similar cases would have to be observed to show that this is normal.

4.3. Vertical Winds at Different Heights

Generally, the vertical winds observed at the two emission wavelengths showed similar behavior except for some isolated cases. This similarity is consistent with the work of *Price et al.* [1995]. The wind velocities estimated from O I 557.7 nm data were consistent with previous results [*Price et al.*, 1995], but the velocities from O I 630.0 nm data were lower. However, the O I 630.0 nm vertical wind velocities can be accepted because the GI-SDI and CRLFPI indicate similar magnitudes. Although it seems strange that the vertical wind accelerated at both altitudes with no time lag in most of the periods, a possible explanation is that the cause of the vertical wind occurs over a wide altitude region. When the vertical winds accelerated simultaneously at both altitudes, auroral luminosities also increased at both wavelengths in many cases. This is evidence that the heating region extends over a wide range of altitude.

As we mentioned in section 2, some events indicated by only the O I 557.7 nm data were not selected for examination. For example, a strong downward wind was observed before and after periods B and M. General characteristics of the O I 557.7 nm temperature estimates were negatively correlated with luminosity, which is consistent with the work of *Price and Jacka* [1991]. Vertical wind velocities estimated from the O I 630.0 nm data also show the same tendency (periods E, G, L, and M), which is consistent with the work of *Innis et al.* [1996].

4.4. Relationship Between Vertical and Horizontal Winds

In our study we observed significant divergence and rotation of the horizontal winds during periods A, B, C, F, G, H, and N, but when active aurora was also present, it was difficult to determine the source of the vertical winds.

It is interesting that there are phase differences between vertical wind periods and the divergence in the horizontal winds. The rotation preceded the downward vertical wind in period A, and large positive divergence and negative rotation were seen after the vertical wind in period G. This time lag may be due to a difference in the observing location: Whereas the vertical winds were observed in small area at the zenith of the observatory, the horizontal winds were measured over the whole sky area. Since most of the events we examined were transient, such a phase lag is reasonable. The relationship between the vertical wind velocity and the rotation of the horizontal wind is not simple to explain. There is usually a large wind shear associated with the rotational region of horizontal wind, and this wind shear might make frictional heating one of the sources of vertical winds.

4.5. Next Step

Our next step will be to use another method to determine the stopping heights of the precipitating particles. For example, *Rees and Luckey* [1974] attempted to determine the characteristic energy and flux by using auroral intensity data obtained from two different wavelengths; we obtained similar data in our observations.

Sipler et al. [1995] attempted to measure vertical wind by applying a triangulation method to data simultaneously obtained at Millstone Hill and Laurel Ridge. This method is good for midlatitude observations but might not work well in the auroral regions because of the high temporal and spatial variation in the emission height. Fundamentally, we need to observe vertical winds underneath the vertical wind events. It is also important to know the vertical wind velocity distribution during each phase of a substorm/storm. Clustered observations obtained with several FPIs will be required to obtain this information, and this will be our next step.

5. Concluding Remarks

Vertical winds in the upper and lower thermosphere were measured with two Fabry-Perot interferometers at Poker Flat, Alaska, from November 1998 to February 1999. Vertical winds were observed by using two emission wavelengths, O I 557.7 nm and O I 630.0 nm, with the CRLFPI. The other instrument, the GI-SDI, provided information on horizontal winds as well as on vertical winds. Fourteen events from four nights were examined, and the relationship between vertical winds and auroral location was statistically analyzed.

Our results show that in 10 of the 14 events, upward vertical winds were observed poleward of an auroral arc, and downward winds were observed equatorward. These results are consistent with previous studies [*Crickmore et al.*, 1991; *Innis et al.*, 1996, 1997]. Our statistical analysis also supported this finding. Thus the vertical wind direction obtained from the O I 630.0 nm emission data may be more significantly related to the O I 557.7 nm auroral distribution than to the O I 630.0 nm distribution. Two of the events, though, showed an opposite relationship between the vertical wind direction and the auroral location.

The vertical winds in the two emission layers generally had similar features. However, in one period (period G) there appeared to be a phase difference between the lower and upper thermospheric vertical winds after a thin but bright auroral arc passed over the observatory.

During many of the events, vertical winds were accompanied by divergences and/or rotations in the horizontal wind field. Most of the vertical wind observations showed a phase difference with the divergences and/or rotations.

Vertical winds can be observed just under the events in the polar region. To obtain information about the vertical wind distribution in the vicinity of an auroral arc, clustered FPI observations are required.

Acknowledgments. We thank June Pelehowski for supporting the operation of the Fabry-Perot interferometers, the meridian-scanning photometer, and the observatory at the Poker Flat Research Range. This study has been supported in part by the U.S.-Japan International Research Project to observe the middle atmosphere, CRL, the Ministry of Posts and Telecommunications, Japan.

Hiroshi Matsumoto thanks H. Rishbeth and D. Rees for their assistance in evaluating this paper.

References

Aruliah, A. L., and D. Rees, The trouble with thermospheric vertical winds: Geomagnetic, seasonal and solar cycle dependence at high latitudes, *J. Atmos. Terr. Phys.*, *57*, 597–609, 1995.

Burnside, R. G., F. A. Herrero, J. W. Meriwether Jr., and J. C. G. Walker, Optical observations of thermospheric dynamics at Arecibo, *J. Geophys. Res.*, *86*, 5532–5540, 1981.

Conde, M., and P. Dyson, Thermospheric vertical winds above Mawson, Antarctica, *J. Atmos. Terr. Phys.*, *57*, 589–596, 1995.

Conde, M., and R. W. Smith, Mapping thermospheric winds in the auroral zone, *Geophys. Res. Lett.*, *22*, 3019–3022, 1995.

Conde, M., and R. W. Smith, "Phase compensation" of a separation scanned, all-sky imaging Fabry-Perot spectrometer for auroral studies, *Appl. Opt.*, *36*, 5441–5450, 1997.

Conde, M., and R. W. Smith, Spatial structure in the thermospheric horizontal wind above Poker Flat, Alaska, during solar minimum, *J. Geophys. Res.*, *103*, 9449–9471, 1998.

Crickmore, R. I., J. R. Dudeney, and A. S. Rodger, Vertical thermospheric winds at the equatorward edge of the auroral oval, *J. Atmos. Terr. Phys.*, *53*, 485–492, 1991.

Innis, J. L., P. A. Greet, and P. L. Dyson, Fabry-Perot spectrometer observations of the auroral oval/polar cap boundary above Mawson, Antarctica, *J. Atmos. Terr. Phys.*, *58*, 1973–1988, 1996.

Innis, J. L., P. L. Dyson, and P. A. Greet, Further observations of the thermospheric vertical wind at the auroral oval/polar cap boundary above Mawson station, Antarctica, *J. Atmos. Terr. Phys.*, *59*, 2009–2022, 1997.

Ishii, M., S. Okano, E. Sagawa, S. Watari, H. Mori, I. Iwamoto, and Y. Murayama, Development of Fabry-Perot interferometers for airglow observations, *Proc. NIPR Symp. Upper Atmos. Phys.*, *10*, 97–108, 1997.

Ishii, M., S. Oyama, S. Nozawa, R. Fujii, E. Sagawa, S. Watari, and H. Shinagawa, Dynamics of neutral wind in the polar region observed with two Fabry-Perot interferometers, *Earth Planets Space*, *51*, 833–844, 1999.

Peteherych, S., G. G. Shepherd, and J. K. Walker, Observation of vertical *E*-region neutral winds in two intense auroral arcs, *Planet. Space Sci.*, *33*, 869–873, 1985.

Price, G. D., and F. Jacka, The influence of geomagnetic activity on the upper mesosphere/lower thermosphere in the auroral zone, I, Vertical winds, *J. Atmos. Terr. Phys.*, *53*, 909–922, 1991.

Price, G. D., R. W. Smith, and G. Hernandez, Simultaneous measurements of large vertical winds in the upper and lower thermosphere, *J. Atmos. Terr. Phys.*, *57*, 631–643, 1995.

Rees, M. H., and D. Luckey, Auroral electron energy derived from ratio of spectroscopic emissions, 1, Model computations, *J. Geophys. Res.*, *79*, 5181–5186, 1974.

Rees, M. H., and R. G. Roble, Excitation of O(^1D) atoms in aurorae and emission of the [OI] 6300-Å line, *Can. J. Phys.*, *64*, 1608–1613, 1986.

Rees, M. H., B. A. Emery, R. C. Roble, and K. Stamnes, Neutral and ion gas heating by auroral electron precipitation, *J. Geophys. Res.*, *88*, 6289–6300, 1983.

Rees, D., R. W. Smith, P. J. Charleton, F. G. McCormac, N. Lloyd, and Å. Steen, The generation of vertical winds and gravity waves at auroral latitudes, I, Observations of vertical winds, *Planet. Space Sci.*, *38*, 667–684, 1984a.

Rees, D., M. F. Smith, and R. Gordon, The generation of vertical thermospheric winds and gravity waves at auroral latitudes, II, Theory and numerical modelling of vertical winds, *Planet. Space Sci.*, *38*, 685–705, 1984b.

Rishbeth, H., T. J. Fuller-Rowell, and D. Rees, Diffusive equilibrium and vertical motion in the thermosphere during a severe magnetic storm: A computational study, *Planet. Space Sci.*, *35*, 1157–1165, 1987.

Sica, R. J., M. H. Rees, G. J. Romick, G. Hernandez, and R. G. Roble, Auroral zone thermospheric dynamics, 1, Averages, *J. Geophys. Res.*, *91*, 3231–3244, 1986.

Sipler, D. P., M. A. Biondi, and M. E. Zipf, Vertical winds in the midlatitude thermosphere from Fabry-Perot interferometer measurements, *J. Atmos. Terr. Phys.*, *57*, 621–629, 1995.

Smith, R. W., and G. Hernandez, Vertical winds in the thermosphere within the polar cap, *J. Atmos. Terr. Phys.*, *57*, 611–620, 1995.

Walterscheid, R. L., L. R. Lyons, and K. E. Taylor, The perturbed neutral circulation in the vicinity of a symmetric stable auroral arc, *J. Geophys. Res.*, *90*, 12,235–12,248, 1985.

M. Conde, M. Krynicki, and R. W. Smith, Geophysical Institute, University of Alaska Fairbanks, 903 Koyukuk Dr., Fairbanks, AK 99775-7320.

M. Ishii, E. Sagawa, and S. Watari, Communications Research Laboratory, 4-2-1 Nukui-Kita, Koganei, Tokyo 184-8795, Japan. (mishii@crl.go.jp)

(Received April 6, 2000; revised August 21, 2000;
accepted October 16, 2000.)